

Optically Active Material Based on $\text{Bi}_2\text{O}_3@Yb^{3+}$, Nd^{3+} with High Intensity of Upconversion Luminescence in the Red and Green Region

D. Artamonov, A. Tsibulnikova, I. Samusev, V. Bryukhanov, A. Kozhevnikov

Abstract—The synthesis and luminescent properties of $\text{Yb}_2\text{O}_3, \text{Nd}_2\text{O}_3@ \text{Bi}_2\text{O}_3$ complex with upconversion generation are discussed in this work. The obtained samples were measured in the visible region of the spectrum under excitation with a wavelength of 980 nm. The studies showed that the obtained complexes have a high degree of stability and intense luminescence in the wavelength range of 400-750 nm. Consideration of the time dependence of the intensity of the upconversion luminescence allowed us to conclude that the enhancement of the intensity occurs in the time interval from 5 to 30 min, followed by the appearance of a stationary mode.

Keywords—Lasers, luminescence, upconversion photonics, rare earth metals.

I. INTRODUCTION

CERAMIC and glass-like materials are currently attracting particular attention due to their unique properties, including high hardness and stability at high temperatures. However, their fabrication process is a complex and multi-step. It requires the using of high temperatures and is often accompanied with the appearance of defects such as cracks and pores [1]-[3]. Therefore, research is now actively underway to develop new technologies to produce these materials. The directions of modern research are modification of glass-like ceramics in order to increase its resistance to external factors and improve its other properties.

Rare earth oxides (REOs) and their solid solutions are very important materials for optical insulators and magneto-optical materials. They provide high optical quality for information and communication technologies, data storage and processing elements, optics, magnetic and laser generation [4], [5]. However, their fabrication process is complex and requires the use of high temperatures. Research is currently underway to develop new technologies to produce these materials with improved properties and increased resistance to external factors.

Materials for optical insulators and magneto-optical materials are REOs and their solid solutions, which are used in information and communication technologies, data storage and processing elements, optics, magnetic and laser generation [6], [7]. However, their fabrication process is complex and requires the use of high temperatures. Ceramic and glass-like materials are also of interest, but the fabrication of ceramics is

challenging, requiring the use of high temperatures and a multi-step process, which can lead to defects [8]-[10]. Therefore, it is important to develop new techniques to produce the materials, for example by doping with Bi_2O_3 or Y_2O_3 compounds to increase the resistance and improve other properties. Bismuth oxide can also be used to modify ceramics due to its low melting point and high reactivity [11].

The purpose of this work is the determination of luminescent features in glassy matrix $\text{Yb}_2\text{O}_3, \text{Nd}_2\text{O}_3@ \text{Bi}_2\text{O}_3$ under excitation into the absorption band of ytterbium ions in the visible and IR ranges under conditions of stationary photoexcitation, investigating the mechanism of energy transfer between Yb^{3+} and Nd^{3+} ions.

II. MATERIALS AND METHODS

Luminescence experiments were performed using a Fluorolog-3 optical system (Horiba and Jobin Yvon, France) equipped with a FL-1073 detector operating in the UV-VIS radiation ranges. An IR laser (model LSR-PS-II) with a continuously adjustable power (0.1-1.0) W and a wavelength of 980 nm was used as an excitation source. A monochromator model M266 (Solar Laser Systems, Belarus) was used to measure luminescence in the IR region.

The synthesis of this material was a multistage thermal process, the final stage of which was high-temperature sintering at $T = 1250^\circ\text{C}$ ($t = 3\text{h}$) in a muffle furnace. Immediately before sintering, the element oxides were subjected to thorough grinding in a mortar. At $T = 900^\circ\text{C}$, the melting process of the mixture began, due to the presence of bismuth oxide, the melting point of which is $T = 850^\circ\text{C}$. The molten solution containing ytterbium oxide and neodymium oxide nanoparticles was cast on the surface. As a result of casting, the sample took the shape of a drop with a diameter of 0.5 cm. The obtained sample was investigated by optical methods in the visible and IR ranges under excitation with a wavelength of 980 nm.

III. RESULTS AND DISCUSSION

Fig. 1 shows the upconversion luminescence of the material under excitation with wavelength of 980 nm.

As can be seen from Fig. 1, the luminescence spectrum in the visible region of $\text{Yb}_2\text{O}_3, \text{Nd}_2\text{O}_3@ \text{Bi}_2\text{O}_3$ was measured at 0.3 W

D. Artamonov, A. Tsibulnikova, I. Samusev, V. Bryukhanov, and A. Kozhevnikov are with the Immanuel Kant Baltic Federal University, Russian Federation (phone: 59-55-95; e-mail: euroset2016ig98@icloud.com).

laser power. The maxima of the luminescence spectrum occur at 525, 545, 555, 555, 655, 665, 695 nm. The transitions between the Yb^{3+} - Nd^{3+} levels correspond with the main ${}^4\text{I}_{9/2} \rightarrow {}^4\text{F}_{5/2}$, ${}^4\text{I}_{9/2} \rightarrow {}^4\text{F}_{9/2}$. Upconversion luminescence bands in the green and red bands are observed in the spectrum [12].

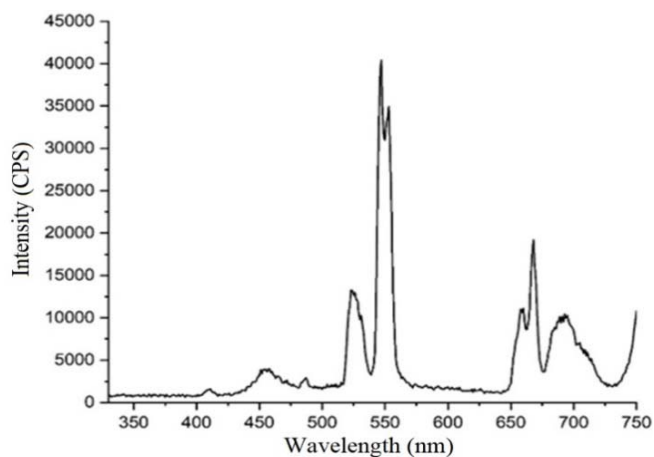


Fig. 1 Luminescence spectra in the visible region of $\text{Yb}_2\text{O}_3,\text{Nd}_2\text{O}_3@\text{Bi}_2\text{O}_3$ at an excitation wavelength of 980 nm

A graph of the intensity dependence vs time of laser exposure is presented in Fig. 2 for $\text{Yb}_2\text{O}_3,\text{Nd}_2\text{O}_3@\text{Bi}_2\text{O}_3$ system.

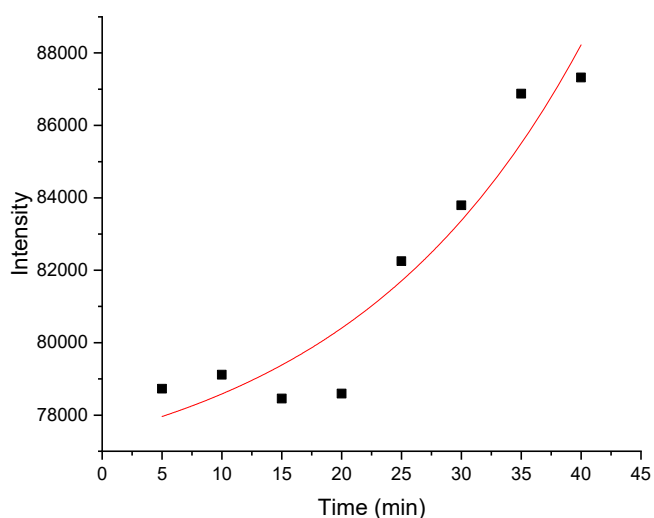


Fig. 2 Dependence of the luminescence maximum at a wavelength of 550 nm on the time of laser excitation at a wavelength of 980 nm

As can be seen from Fig. 2, the intensity enhancement occurs in the time interval from 5 min up to 30 min followed by a stationary mode. Thus, it can be seen that the luminescence intensity is a stationary process of energy accumulation at the ${}^2\text{G}_{9/2}$ level, since the intensity does not practically change with power. For the other wavelengths, a nonlinear dependence is observed, which is apparently due to the influence of concomitant parallel transitions on each electron transition under consideration and possible additional energy transfer from the upper levels.

The exponential growth of the high-efficiency red UCL may

also indicate a sufficiently high degree of stability of the obtained material. In this context, we believe the stability is due to the Bi_2O_3 shell, which seems to delay the upconversion radiation and scatter the absorbed IR radiation in the volume of the material (drop), forming a kind of resonator, which provides irradiation of a large number of neighboring atoms.

Further, Raman spectra of $\text{Bi}_2\text{O}_3@\text{Yb}^{3+}, \text{Nd}^{3+}$ in Yb^{3+} to Nd^{3+} concentration ($m_{\text{Yb}_2\text{O}_3} = 0,56\text{g}; m_{\text{Nd}_2\text{O}_3} = 0,24\text{g}$) and ($m_{\text{Yb}_2\text{O}_3} = 0,08\text{g}; m_{\text{Nd}_2\text{O}_3} = 0,72\text{g}$) were considered. It should be noted that the ytterbium oxide phase remains constant under the two sintering regimes (cubic lattice type Ia 3) [13].

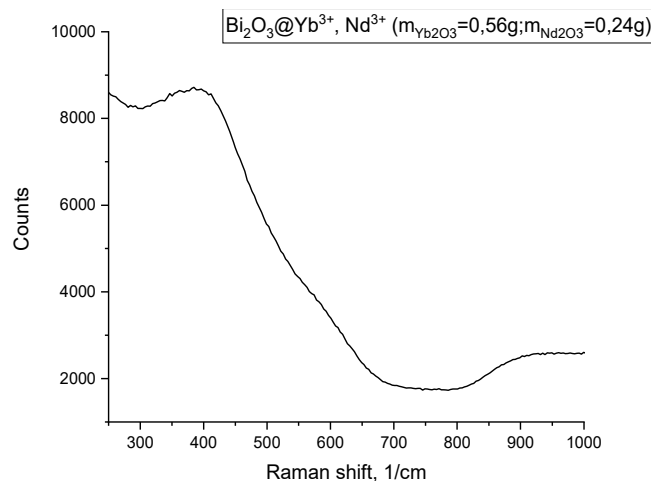


Fig. 3 Raman spectrum of $\text{Bi}_2\text{O}_3@\text{Yb}^{3+}, \text{Nd}^{3+}$ ($m_{\text{Yb}_2\text{O}_3} = 0,56\text{g}; m_{\text{Nd}_2\text{O}_3} = 0,24\text{g}$)

Thus, from the spectrum presented in Fig. 3, the characteristic peaks of Nd-O bond vibrations at frequency of $\nu = 400 \text{ cm}^{-1}$ corresponding to E_g Raman modes are observed [14]. The presence of this peak indicates a C-type cubic lattice with spatial symmetry Ia3 for Nd_2O_3 powder.

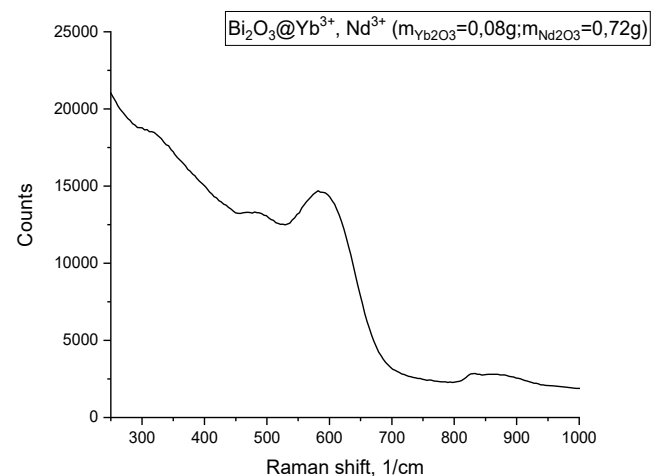


Fig. 4 Raman spectrum of $\text{Bi}_2\text{O}_3@\text{Yb}^{3+}, \text{Nd}^{3+}$ ($m_{\text{Yb}_2\text{O}_3} = 0,08\text{g}; m_{\text{Nd}_2\text{O}_3} = 0,72\text{g}$)

The vibration maximum of annealed Nd_2O_3 at temperature $T = 1200 \text{ }^\circ\text{C}$ is located at the frequency of $\nu = 605 \text{ cm}^{-1}$ (e.g., mode). This neodymium oxide Nd_2O_3 is characterized by the C-

form [15]-[17].

It is important to note that in the mixture of oxides $\text{Nd}_2\text{O}_3/\text{Yb}_2\text{O}_3$ after annealing at $T = 750^\circ\text{C}$, there is an increase in the intensity of vibrational bands corresponding to frequencies 450 cm^{-1} and 605 cm^{-1} in the spectrum. This is due to the overlap of vibrational spectra in this region for Nd_2O_3 and Yb_2O_3 and algebraic summation of the amplitude of vibrations and oscillation strength of Nd-O_3 and Yb-O bonds [18]-[20].

Thus, based on the results of vibrational spectroscopy, it can be concluded that the phase of ytterbium oxide in $\text{Yb}_2\text{O}_3, \text{Nd}_2\text{O}_3 @ \text{Bi}_2\text{O}_3$ medium remains constant and undergoes insignificant changes, which is extremely important for the consideration of Yb^{3+} ions as an energy donor for

photoactivation of Nd^{3+} ions under excitation into the electronic absorption band of Yb^{3+} . To establish the presence of luminescent properties in ytterbium oxide, the luminescence spectra of $\text{Yb}_2\text{O}_3 @ \text{Bi}_2\text{O}_3$ and $\text{Yb}_2\text{O}_3, \text{Nd}_2\text{O}_3 @ \text{Bi}_2\text{O}_3$ medium were measured.

X-ray diffraction analysis of Bi_2O_3 in powder and droplet was carried out to investigate their morphological characteristics, which affect the media values for rare earth elements. Fig. 5 shows the X-ray diffraction pattern of Bi_2O_3 powder.

Bismuth oxide has a monoclinic lattice with the space group of a $P 21/c$ (card No. 2-498). The unit cell parameters are: $a = 5.83\text{ \AA}$, $b = 8.14\text{ \AA}$, $c = 7.48\text{ \AA}$, $\alpha = 90^\circ$, $\beta = 67.7^\circ$, $\gamma = 90^\circ$.

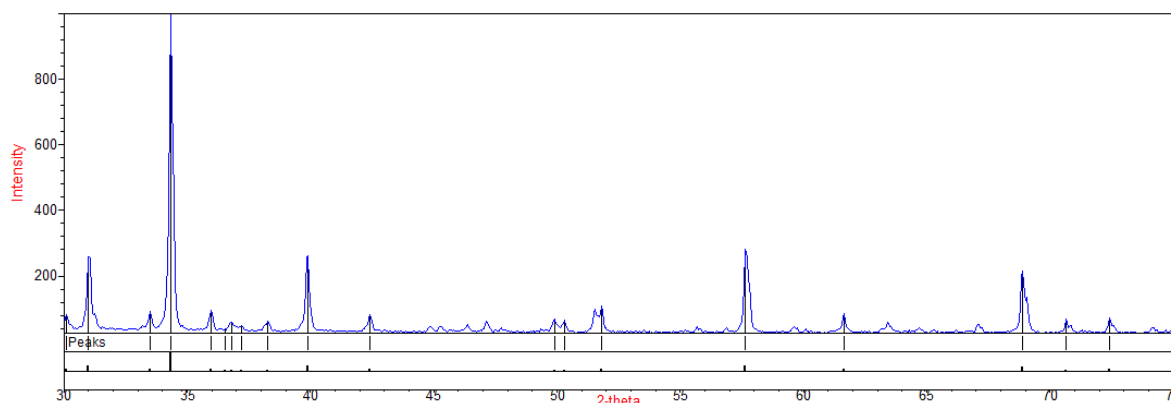


Fig. 5 X-ray diffraction pattern of the Bi_2O_3

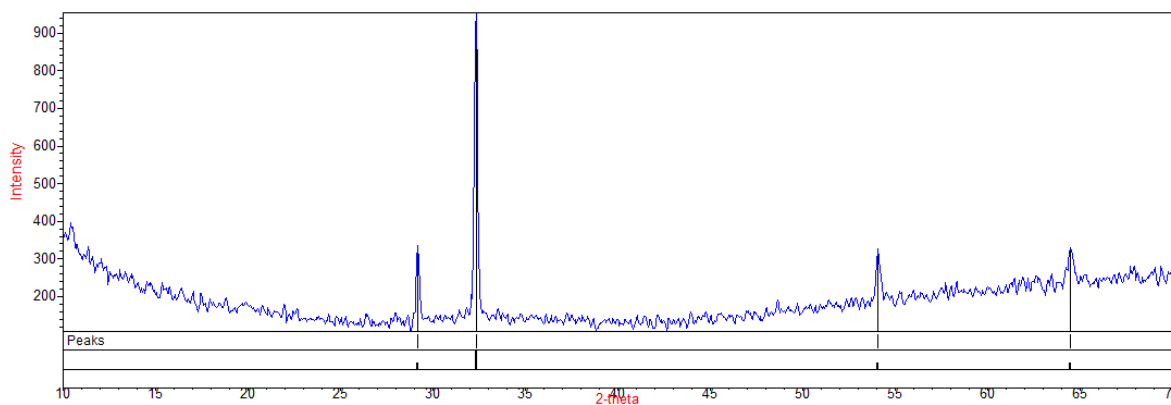


Fig. 6 X-Ray diffraction pattern of the Bi_2O_3 -drop

As can be seen from Fig. 6, Bi_2O_3 in the drop at annealing temperature of 1250°C has an amorphous state, since it has no obvious X-ray scattering peaks and therefore is a good medium for the study of upconversion processes involving ions of rare earth elements.

IV. CONCLUSION

Based on the results of vibrational spectroscopy, it was found that in the Raman spectrum of the mixture of oxides $\text{Nd}_2\text{O}_3/\text{Yb}_2\text{O}_3$ after sintering at $T = 750^\circ\text{C}$, there is an increase in the intensity of vibrational bands corresponding to frequencies 360 cm^{-1} and 605 cm^{-1} , due to the spectral overlap of bands Nd_2O_3 and Yb_2O_3 . It was also found that the phase of

ytterbium oxide in the medium of $\text{Yb}_2\text{O}_3, \text{Nd}_2\text{O}_3 @ \text{Bi}_2\text{O}_3$ remains constant. According to the data of luminescence analysis it was shown that the investigated material $\text{Yb}_2\text{O}_3, \text{Nd}_2\text{O}_3 @ \text{Bi}_2\text{O}_3$ has upconversion luminescence with high optical stability and has no photochemical burnout. It is proved that the upconversion transitions in the red and green regions are due to the dipole-dipole mechanism of energy transfer with simultaneous excitation of a pair of ytterbium ions in the absorption band. It is also shown that the bismuth oxide shell provides stability of the process of internal reabsorption of IR energy under conditions of constant photoexcitation of ytterbium ions.

ACKNOWLEDGMENTS

The reported study was funded by the Ministry of Science and Higher Education of the Russian Federation (FZWM-2024-0010).

REFERENCES

- [1] Patil, A.S.; Patil, A. V.; Dighavkar, C.G.; Adole, V.A.; Tupe, U.J. Synthesis Techniques and Applications of Rare Earth Metal Oxides Semiconductors: A Review. *Chem. Phys. Lett.* 2022, 796, 139555, doi:10.1016/J.CPLETT.2022.139555.
- [2] Furuse, H.; Yasuhara, R. Magneto-Optical Characteristics of Holmium Oxide (Ho₂O₃) Ceramics. *Opt. Mater. Express* 2017, 7, 827, doi:10.1364/ome.7.000827.
- [3] Balaram, V. Rare Earth Elements: A Review of Applications, Occurrence, Exploration, Analysis, Recycling, and Environmental Impact. *Geosci. Front.* 2019, 10, 1285–1303, doi:10.1016/j.gsf.2018.12.005.
- [4] Hossain, M.K.; Rubel, M.H.K.; Akbar, M.A.; Ahmed, M.H.; Haque, N.; Rahman, M.F.; Hossain, J.; Hossain, K.M. A Review on Recent Applications and Future Prospects of Rare Earth Oxides in Corrosion and Thermal Barrier Coatings, Catalysts, Tribological, and Environmental Sectors. *Ceram. Int.* 2022, 48, 32588–32612, doi:https://doi.org/10.1016/j.ceramint.2022.07.220.
- [5] Tan, Y.; Liao, W.; Zeng, S.; Jia, P.; Teng, Z.; Zhou, X.; Zhang, H. Microstructures, Thermophysical Properties and Corrosion Behaviours of Equiatomic Five-Component Rare-Earth Monosilicates. *J. Alloys Compd.* 2022, 907, 164334, doi: https://doi.org/10.1016/j.jallcom.2022.164334.
- [6] Singh, A.K.; Kutty, T.R.G.; Sinha, S. Pulsed Laser Deposition of Corrosion Protective Yttrium Oxide (Y₂O₃) Coating. *J. Nucl. Mater.* 2012, 420, 374–381, doi:https://doi.org/10.1016/j.jnucmat.2011.10.028.
- [7] Bahamirian, M.; Hadavi, S.M.M.; Farvizi, M.; Rahimpour, M.R.; Keyvani, A. Phase Stability of ZrO₂ 9.5Y₂O₃ 5.6Yb₂O₃ 5.2Gd₂O₃ Compound at 1100 °C and 1300 °C for Advanced TBC Applications. *Ceram. Int.* 2019, 45, 7344–7350, doi: https://doi.org/10.1016/j.ceramint.2019.01.018.
- [8] Jeon, H.; Lee, I.; Oh, Y. Changes in High-Temperature Thermal Properties of Modified YSZ with Various Rare Earth Doping Elements. *Ceram. Int.* 2022, 48, 8177–8185, doi: https://doi.org/10.1016/j.ceramint.2021.12.020.
- [9] Adachi, G.Y.; Imanaka, N. The Binary Rare Earth Oxides. *Chem. Rev.* 1998, 98, 1479–1514, doi:10.1021/cr940055h.
- [10] Novák, O.; Miura, T.; Smrž, M.; Chyla, M.; Nagisetty, S.S.; Mužík, J.; Linnemann, J.; Turčičová, H.; Jambunathan, V.; Slezák, O.; et al. Status of the High Average Power Diode-Pumped Solid State Laser Development at HiLASE. *Appl. Sci.* 2015, 5, 637–665, doi:10.3390/app5040637.
- [11] Cheng, Y.-L.; Lee, C.-Y.; Huang, Y.-L.; Buckner, C.A.; Lafrenie, R.M.; Dénommée, J.A.; Caswell, J.M.; Want, D.A.; Gan, G.G.; Leong, Y.C.; et al. From the Laser Plume to the Laser Ceramics. *Intech* 2016, 11, 13.
- [12] Zhang, Y.; Hu, S.; Tian, T.; Xiao, X.; Chen, Y.; Zhang, Y.; Xu, J. Growth and Spectral Properties of Er³⁺ and Yb³⁺ Co-Doped Bismuth Silicate Single Crystal. *Crystals* 2022, 12, 1532, doi:10.3390/cryst12111532.
- [13] Gorbachenya, K.N.; Yasukevich, A.S.; Lazarchuk, A.I.; Kisel, V.E.; Kuleshov, N. V.; Volkova, E.A.; Maltsev, V. V.; Koporulina, E. V.; Yapaskurt, V.O.; Kuzmin, N.N.; et al. Growth and Spectroscopy of Yb:YMGb₅O₁₀ Crystal. *Crystals* 2022, 12, 1–11, doi:10.3390/cryst12070986.
- [14] Piconi, C.; Maccauro, G. Zirconia as a Ceramic Biomaterial. *Biomaterials* 1999, 20, 1–25, doi:https://doi.org/10.1016/S0142-9612(98)00010-6.
- [15] Moqbel, N.M.; Al-Akhali, M.; Wille, S.; Kern, M. Influence of Aging on Biaxial Flexural Strength and Hardness of Translucent 3Y-TZP. *Materials (Basel)*. 2020, 13, 27, doi:10.3390/ma13010027.
- [16] Kozlovskiy, A.L.; Seitbayev, A.S.; Borgekov, D.B.; Zdorovets, M. V. Study of the Structural, Optical and Strength Properties of Glass-like (1-x)ZnO-0.25Al₂O₃-0.25WO₃-xBi₂O₃ Ceramics. *Crystals* 2022, 12, 1–14, doi:10.3390/cryst12111527.
- [17] Yi, H.; Che, J.; Liang, G.; Liu, X. Effect of Rare Earth Elements on Stability and Sintering Resistance of Tetragonal Zirconia for Advanced Thermal Barrier Coatings. *Crystals* 2021, 11, doi:10.3390/cryst11030287.
- [18] Secu, M.; Secu, C.E. Processing and Optical Properties of Eu-Doped Chloroborate Glass-Ceramic. *Crystals* 2020, 10, 1–12, doi:10.3390/cryst10121101.
- [19] Cao, J.; Wondraczek, L.; Wang, Y.; Wang, L.; Li, J.; Xu, S.; Peng, M.

- Ultrabroadband Near-Infrared Photoemission from Bismuth-Centers in Nitridated Oxide Glasses and Optical Fiber. *ACS Photonics* 2018, 5, 4393–4401, doi:10.1021/acsp Photonics.8b00814.
- [20] Teibulnikova, A. V.; Myslitskaya, N.A.; Slezhkin, V.A.; Bruykanov, V. V.; Samusev, I.G.; Lyatun, I.I. Upconversion Luminescence Enhancement of the Ytterbium Oxide with Gold Nanoparticles on Anodized Titanium Surface. *J. Lumin.* 2022, 251, 119157, doi:10.1016/j.jlumin.2022.119157.